Low-voltage magnetoresistance in silicon

ARISING FROM C. H. Wan, X. Z. Zhang, X. L. Gao, J. M. Wang & X. Y. Tan *Nature* **477,** 304–307 (2011)

Magnetoresistance exhibited by non-magnetic semiconductors has attracted much attention[1–13]. In particular, Wan *et al.* reported room-temperature magnetoresistance in silicon to reach 10% at 0.07 T and 150,000% at 7 T—"an intrinsically spatial effect"[12]. Their supply voltage was approximately 10 V (ref. 12), which is low and approaches the industrial requirement[14]. However, we have found their large magnetoresistance values to be experimental artefacts caused by their method of measurement. The true room-temperature magnetoresistance of the devices described in ref. 12 is low with a magnetic field of up to 7 T and a supply voltage of around 10 V and hence these devices cannot offer large magnetoresistance with low supply voltage to industry. There is a Reply to this Brief Communication Arising by Zhang, X. Z., Wan, C. H., Gao, X. L., Wang, J. M. & Tan, X. Y. *Nature* **501,** http://dx.doi.org/10.1038/nature12590 (2013).

Wan *et al.*[12] measured two types of In/SiO_2/Si/SiO_2/In devices using a Keithley 2400 sourcemeter as both a current source and a voltage meter (which we refer to here as method 1), and obtained large magnetoresistance values of up to 10% at 0.07 T and 150,000% at 7 T. We fabricated two devices with the same structures as those of ref. 12 and performed method 1 using them. Their voltage–current (V–I) curves can be divided into different regions with different resistances, just as in the results of ref. 12. Wan *et al.*[12] claim that injection of minority carriers into silicon causes a p–n junction and the changes in resistance, that large magnetoresistance occurs with applied current in one of the regions (referred as to the transition region), and that the magnetic-field dependence of the magnetoresistance in the transition region is different from those in the other regions. However, when we used another method (here called method 2) with unchanged measuring parameters and different instruments on the devices, the V–I characteristics without the transition region were obtained. The only difference between the two methods is that in method 2 we used the Keithley 2400 only as the current source, with an independent voltmeter (Keithley 2182) as the voltage meter.

Further, we performed both methods on two circuits composed of linear resistors, which were used to simulate the devices. The results indicate that in method 1 the Keithley 2400 itself interferes with the measurement of the specimen and cannot give correct voltage values when the applied current exceeds a certain value and falls in the transition region. Because ref. 12 claims that large magnetoresistances were measured when I was in the transition region, magnetoresistance was defined as $[R(B) - R(B = 0)]/R(B = 0)$ and $R = V/I$, we conclude that the large magnetoresistance values are really experimental artefacts caused by the interference of the sourcemeter. Method 2 is valid. Using it, we obtained magnetoresistance values for the two devices with supply voltages of 6.7–72 V and 0.79–50 V, respectively. The values are all low and the magnetic-field dependence at all applied currents is the same (above 2 T the field dependence is linear); the magnetoresistance does not exhibit any signs of saturation at fields up to 7 T. The linear dependence without magnetoresistance saturation is the same as for inhomogeneity-induced magnetoresistance[7–9].

Jun Luo[1], Peisen Li[2], Sen Zhang[2], Hongyu Sun[1], Hongping Yang[1] & Yonggang Zhao[2]

[1]Beijing National Center for Electron Microscopy, Laboratory of Advanced Materials, Department of Materials Science and Engineering, Tsinghua University, Beijing 100084, China.
email: jluo@mail.tsinghua.edu.cn

[2]Department of Physics and State Key Laboratory of Low-Dimensional Quantum Physics, Tsinghua University, Beijing 100084, China.

Received 20 September 2012; accepted 16 August 2013.

1. Smith, R. A. *Semiconductors* 2nd edn, Ch. 5 (Cambridge Univ. Press, 1978).
2. Popović, R. S. *Hall Effect Devices* Ch. 3 (IOP Publishing, 1991).
3. Xu, R. *et al.* Large magnetoresistance in non-magnetic silver chalcogenides. *Nature* **390,** 57–60 (1997).
4. Solin, S. A., Thio, T., Hines, D. R. & Heremans, J. J. Enhanced room-temperature geometric magnetoresistance in inhomogeneous narrow-gap semiconductors. *Science* **289,** 1530–1532 (2000).
5. Lee, M., Rosenbaum, T. F., Saboungi, M.-L. & Schnyders, H. S. Band-gap tuning and linear magnetoresistance in the silver chalcogenides. *Phys. Rev. Lett.* **88,** 066602 (2002).
6. Husmann, A. *et al.* Megagauss sensors. *Nature* **417,** 421–424 (2002).
7. Parish, M. M. & Littlewood, P. B. Non-saturating magnetoresistance in heavily disordered semiconductors. *Nature* **426,** 162–165 (2003).
8. Hu, J. S. & Rosenbaum, T. F. Classical and quantum routes to linear magnetoresistance. *Nature Mater.* **7,** 697–700 (2008).
9. Delmo, M. P., Yamamoto, S., Kasai, S., Ono, T. & Kobayashi, K. Large positive magnetoresistive effect in silicon induced by the space-charge effect. *Nature* **457,** 1112–1115 (2009).
10. Delmo, M. P., Kasai, S., Kobayashi, K. & Ono, T. Current-controlled magnetoresistance in silicon in non-Ohmic transport regimes. *Appl. Phys. Lett.* **95,** 132106 (2009).
11. Schoonus, J. J. H. M., Haazen, P. P. J., Swagten, H. J. M. & Koopmans, B. Unravelling the mechanism of large room-temperature magnetoresistance in silicon. *J. Phys. D* **42,** 185011 (2009).
12. Wan, C. H., Zhang, X. Z., Gao, X. L., Wang, J. M. & Tan, X. Y. Geometrical enhancement of low-field magnetoresistance in silicon. *Nature* **477,** 304–307 (2011).
13. Porter, N. A. & Marrows, C. H. Linear magnetoresistance in *n*-type silicon due to doping density fluctuations. *Sci. Rep.* **2,** 565 (2012).
14. Allan, A. *et al.* 2011 edn, http://www.itrs.net/Links/2011ITRS/Home2011.htm (2011).

Author Contributions J.L. designed the research blueprint, performed the experiments and data analysis, and wrote the manuscript. P.L. and S.Z. assisted in the magnetoresistance measurement and data analysis. H.S. and H.Y. assisted in the data collection. Y.Z. supervised the magnetoresistance measurement and contributed to the data analysis and manuscript writing.

Competing Financial Interests Declared none.

doi:10.1038/nature12589

Zhang *et al.* reply

REPLYING TO J. Luo *et al. Nature* **501,** http://dx.doi.org/10.1038/nature12589 (2013)

We agree with Luo *et al.*[1] that the magnetoresistance effects that we reported[2] were dependent on the method used to measure them. The reason that there is a difference in the results depending on whether method 1 or method 2 is used (adopting the measurement notation of ref. 1) is that there are two voltage-stabilizing diodes in the Keithley 2400 instrument we used. We were unaware that when this instrument was used both as current source and voltmeter, one diode connected the input port of the current source to the input port of the

nature COMMUNICATIONS

ARTICLE

Received 9 May 2013 | Accepted 7 Oct 2013 | Published 30 Oct 2013

DOI: 10.1038/ncomms3719 OPEN

Confinement of pyridinium hemicyanine dye within an anionic metal-organic framework for two-photon-pumped lasing

Jiancan Yu[1,*], Yuanjing Cui[1,*], Hui Xu[1], Yu Yang[1], Zhiyu Wang[1], Banglin Chen[1,2] & Guodong Qian[1]

Two-photon-pumped dye lasers are very important because of their applications in wavelength up-conversion, optical data storage, biological imaging and photodynamic therapy. Such lasers are very difficult to realize in the solid state because of the aggregation-caused quenching. Here we demonstrate a new two-photon-pumped micro-laser by encapsulating the cationic pyridinium hemicyanine dye into an anionic metal-organic framework (MOF). The resultant MOF⊃dye composite exhibits significant two-photon fluorescence because of the large absorption cross-section and the encapsulation-enhanced luminescent efficiency of the dye. Furthermore, the well-faceted MOF crystal serves as a natural Fabry–Perot resonance cavity, leading to lasing around 640 nm when pumped with a 1064-nm pulse laser. This strategy not only combines the crystalline benefit of MOFs and luminescent behaviour of organic dyes but also creates a new synergistic two-photon-pumped lasing functionality, opening a new avenue for the future creation of solid-state photonic materials and devices.

[1] State Key Laboratory of Silicon Materials, Department of Materials Science and Engineering, Cyrus Tang Center for Sensor Materials and Applications, Zhejiang University, Hangzhou 310027, China. [2] Department of Chemistry, University of Texas at San Antonio, San Antonio, Texas 78249-0698, USA. * These authors contributed equally to this work. Correspondence and requests for materials should be addressed to B.C (email: banglin.chen@utsa.edu) or to G.Q. (email: gdqian@zju.edu.cn).

LETTER

doi:10.1038/nature13829

Solution-processed, high-performance light-emitting diodes based on quantum dots

Xingliang Dai[1], Zhenxing Zhang[2], Yizheng Jin[1], Yuan Niu[2], Hujia Cao[2], Xiaoyong Liang[1], Liwei Chen[3], Jianpu Wang[4] & Xiaogang Peng[2]

Solution-processed optoelectronic and electronic devices are attractive owing to the potential for low-cost fabrication of large-area devices and the compatibility with lightweight, flexible plastic substrates. Solution-processed light-emitting diodes (LEDs) using conjugated polymers or quantum dots as emitters have attracted great interest over the past two decades[1,2]. However, the overall performance of solution-processed LEDs[2–5]—including their efficiency, efficiency roll-off at high current densities, turn-on voltage and lifetime under operational conditions—remains inferior to that of the best vacuum-deposited organic LEDs[6–8]. Here we report a solution-processed, multilayer quantum-dot-based LED with excellent performance and reproducibility. It exhibits colour-saturated deep-red emission, sub-bandgap turn-on at 1.7 volts, high external quantum efficiencies of up to 20.5 per cent, low efficiency roll-off (up to 15.1 per cent of the external quantum efficiency at 100 mA cm^{-2}), and a long operational lifetime of more than 100,000 hours at 100 cd m^{-2}, making this device the best-performing solution-processed red LED so far, comparable to state-of-the-art vacuum-deposited organic LEDs[2–8]. This optoelectronic performance is achieved by inserting an insulating layer between the quantum dot layer and the oxide electron-transport layer to optimize charge balance in the device and preserve the superior emissive properties of the quantum dots. We anticipate that our results will be a starting point for further research, leading to high-performance, all-solution-processed quantum-dot-based LEDs ideal for next-generation display and solid-state lighting technologies.

Quantum dots are solution-processable semiconductor nanocrystals[9–11] that promise size-tunable emission wavelengths, narrow emission linewidths, near-unity-photoluminance quantum yield and inherent photophysical stability. As inorganic crystalline emission centres, quantum dots are expected to be promising candidates to overcome stability problems of both polymer LEDs and small-molecule organic LEDS (OLEDs), such as drastic efficiency roll-off at high current densities and low operational lifetime. To fully exploit the superior properties of quantum dots, a number of quantum-dot-based LED (QLED) structures were developed and various materials, including small molecules, conjugated polymers and inorganic oxides, were explored as charge-transport interlayers[3,12–20].

Our device (Fig. 1a, b) consists of multiple layers of, in the following order, indium tin oxide (ITO), poly(ethylenedioxythiophene):polystyrene sulphonate (PEDOT:PSS, 35 nm), poly (*N*,*N*′-bis(4-butylphenyl)-*N*,*N*′-bis(phenyl)-benzidine) (poly-TPD, 30 nm), poly(9-vinlycarbazole)

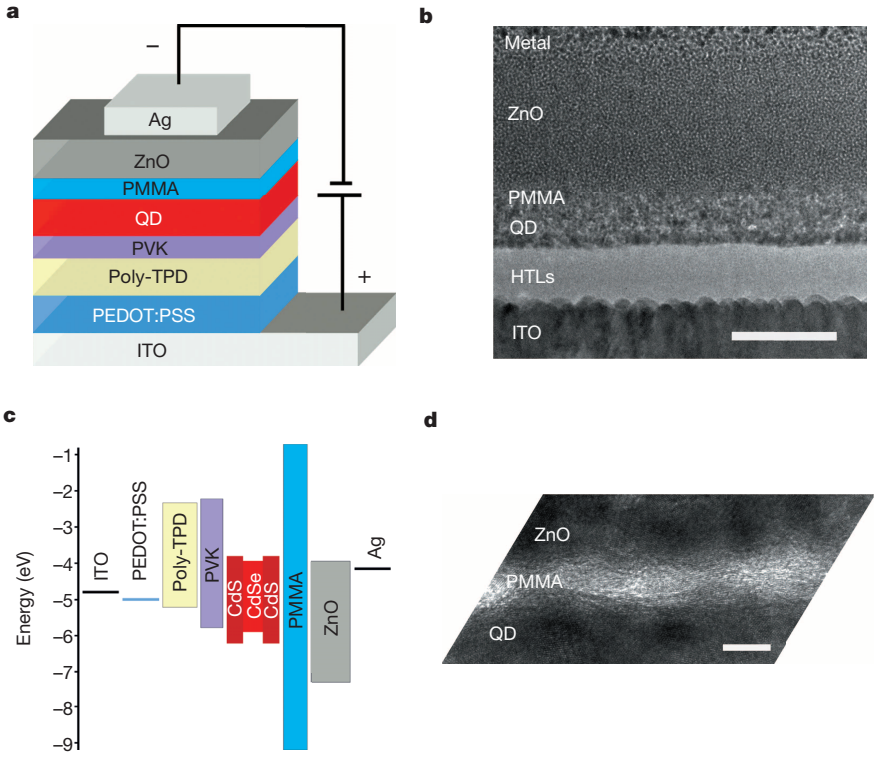

Figure 1 | Multilayer QLED device. **a**, Device structure. **b**, Cross-sectional transmission electron microscopy image showing the multiple layers of material with distinct contrast. Scale bar, 100 nm. The PMMA layer is evident only when the cross-sectional sample is sufficiently thin (**d**) because the neighbouring quantum dot layer and the ZnO layer can obstruct the imaging of the PMMA layer. HTL, hole-transport interlayer. **c**, Flat-band energy level diagram. **d**, High-magnification transmission electron microscopy image of an extremely thin cross-sectional sample revealing the presence of the PMMA layer between the ZnO layer and the quantum dot layer. Scale bar, 5 nm.

[1]Center for Chemistry of High-Performance & Novel Materials, State Key Laboratory of Silicon Materials, Cyrus Tang Center for Sensor Materials and Applications, School of Materials Science and Engineering, Zhejiang University, Hangzhou 310027, China. [2]Center for Chemistry of High-Performance & Novel Materials, Department of Chemistry, Zhejiang University, Hangzhou 310027, China. [3]i-Lab, Suzhou Institute of Nano-Tech and Nano-Bionics, Chinese Academy of Sciences, 398 Ruoshui Road, Suzhou Industrial Park, Suzhou 215123, China. [4]Key Laboratory of Flexible Electronics (KLOFE) & Institute of Advanced Materials (IAM), National Jiangsu Synergistic Innovation Center for Advanced Materials (SICAM), Nanjing Tech University (NanjingTech), 30 South Puzhu Road, Nanjing 211816, China.

nature COMMUNICATIONS

ARTICLE

Received 31 Aug 2014 | Accepted 15 Jan 2015 | Published 19 Feb 2015

DOI: 10.1038/ncomms7293 OPEN

Exploring atomic defects in molybdenum disulphide monolayers

Jinhua Hong[1,*], Zhixin Hu[2,*], Matt Probert[3], Kun Li[4], Danhui Lv[1], Xinan Yang[5], Lin Gu[5], Nannan Mao[6,7], Qingliang Feng[6], Liming Xie[6], Jin Zhang[7], Dianzhong Wu[8], Zhiyong Zhang[8], Chuanhong Jin[1], Wei Ji[2,9], Xixiang Zhang[4], Jun Yuan[1,3] & Ze Zhang[1]

Defects usually play an important role in tailoring various properties of two-dimensional materials. Defects in two-dimensional monolayer molybdenum disulphide may be responsible for large variation of electric and optical properties. Here we present a comprehensive joint experiment–theory investigation of point defects in monolayer molybdenum disulphide prepared by mechanical exfoliation, physical and chemical vapour deposition. Defect species are systematically identified and their concentrations determined by aberration-corrected scanning transmission electron microscopy, and also studied by *ab-initio* calculation. Defect density up to $3.5 \times 10^{13}\,cm^{-2}$ is found and the dominant category of defects changes from sulphur vacancy in mechanical exfoliation and chemical vapour deposition samples to molybdenum antisite in physical vapour deposition samples. Influence of defects on electronic structure and charge-carrier mobility are predicted by calculation and observed by electric transport measurement. In light of these results, the growth of ultra-high-quality monolayer molybdenum disulphide appears a primary task for the community pursuing high-performance electronic devices.

[1] State Key Laboratory of Silicon Materials, Key Laboratory of Advanced Materials and Applications for Batteries of Zhejiang Province, School of Materials Science and Engineering, Zhejiang University, Hangzhou, Zhejiang 310027, China. [2] Beijing Key Laboratory of Optoelectronic Functional Materials and Micro-Nano Devices, Department of Physics, Renmin University of China, Beijing 100872, China. [3] Department of Physics, University of York, Heslington, York YO10 5DD, UK. [4] Advanced Nanofabrication, Imaging and Characterization Core Lab, King Abdullah University of Science and Technology (KAUST), Thuwal 239955, Kingdom of Saudi Arabia. [5] Instituteof Physics, Chinese Academy of Sciences, c/o Collaborative Innovation Center of Quantum Matter, Beijing 100190, China. [6] CAS Key Laboratory of Standardization and Measurement for Nanotechnology, National Center for Nanoscience and Technology, Beijing 100190, China. [7] Center for Nanochemistry, Beijing National Laboratory for Molecular Sciences, Key Laboratory for the Physics and Chemistry of Nanodevices, State Key Laboratory for Structural Chemistry of Unstable and Stable Species, College of Chemistry and Molecular Engineering, Peking University, Beijing 100871, China. [8] Key Laboratory for the Physics and Chemistry of Nanodevices and Department of Electronics, Peking University, Beijing 100871, China. [9] Department of Physics and Astronomy, Collaborative Innovation Center of Advanced Microstructures, Shanghai Jiao Tong University, Shanghai 200240, China. * These authors contributed equally to this work. Correspondence and requests for materials should be addressed to C.J. (email: chhjin@zju.edu.cn) or to W.J. (email: wji@ruc.edu.cn) or to J.Y. (email: jun.yuan@york.ac.uk).